

MOL 8685

## Title Page

# **The CCR5 Receptor-based mechanism of action of 873140, a potent allosteric non-competitive HIV entry-inhibitor**

Christian Watson , Stephen Jenkinson, Wieslaw Kazmierski, and Terry Kenakin

Assay Development and Compound Profiling (CW, TK)

Department of Biochemical and Analytical Pharmacology (SJ)

Department of Medicinal Chemistry (WK)

GlaxoSmithKline Research and Development  
5 Moore Drive  
Research Triangle Park, NC 27709

MOL 8685

## Running Title Page

**Running Title:** Blockade of CCR5-mediated HIV entry

**Corresponding Author: Terry Kenakin**

Assay Development and Compound Profiling (CW, TK)

GlaxoSmithKline Research and Development

5 Moore Drive

Research Triangle Park, NC 27709

Tele: 919-483-6192

Email: [Terry.P.Kenakin@gsk.com](mailto:Terry.P.Kenakin@gsk.com)

Text Pages:	58
Tables :	3
Figures :	11
References :	53
Abstract # words :	246
Introduction # words:	361
Discussion # words:	2065

## Abbreviations:

**Mip-1 $\alpha$**  Macrophage Inflammatory Protein 1-alpha (standard nomenclature  
CCL3, also known as LD78)

**RANTES** Regulated on Activation, Normal T cell Expressed and Secreted  
(standard nomenclature for this chemokine is CCL5)

MOL 8685

- Sch-C** (Z)-(4-bromophenyl){1'-[(2,4-dimethyl-1-oxido-3-pyridinyl)carbonyl]-4'-methyl-1,4'-bipiperidin-4-yl}methanone O-ethyloxime
- Sch-D** 4,6-dimethyl-5-{[4-methyl-4-((3S)-3-methyl-4-{(1R)-2-(methyloxy)-1-[4-(trifluoromethyl)phenyl]ethyl}-1-piperazinyl)-1-piperidinyl]carbonyl}pyrimidine
- UK 427,857** 4,4-difluoro-*N*-((1*S*)-3-{(3-*endo*)-3-[3-methyl-5-(1-methylethyl)-4*H*-1,2,4-triazol-4-yl]-8-azabicyclo[3.2.1]oct-8-yl}-1-phenylpropyl)cyclohexanecarboxamide
- TAK779** *N,N*-dimethyl-*N*-[4-[[[2-(4-methylphenyl)-6,7-dihydro-5*H*-benzocyclohepten-8-yl]carbonyl]amino]benzyl]tetrahydro-2*H*-pyran-4-aminium chloride.
- 873140** 4-{[4-({(3*R*)-1-butyl-3-[(*R*)-cyclohexyl(hydroxy)methyl]-2,5-dioxo-1,4,9-triazaspiro[5.5]undec-9-yl)methyl]phenyl}oxy}benzoic acid hydrochloride
- UCB35625** 1-Cycloheptylmethyl-4-{[1-(2,7-dichloro-9*H*-xanthen-9-yl)-methanoyl]-amino}-1-methyl-piperidinium,
- I-TAC** interferon-inducible T cell  $\alpha$  chemoattractant
- IP-10** 10-kDa interferon-inducible protein

MOL 8685

## Abstract

### **The CCR5 Receptor-based mechanism of action of 873140, a potent allosteric non-competitive HIV entry-inhibitor**

873140 is a potent non-competitive allosteric antagonist of the CCR5 receptor ( $pK_B = 8.6 \pm 0.07$  ; 95 % c.l. = 8.5 to 8.8) with concomitantly potent antiviral effects for HIV-1. In this paper, the receptor-based mechanism of action of 873140 is compared to four other non-competitive allosteric antagonists of CCR5. While Sch-C, Sch-D, UK-427,857, and TAK779 blocked both the binding of the chemokines  $^{125}\text{I}$ -MIP-1 $\alpha$  (also known as  $^{125}\text{I}$ -CCL3,  $^{125}\text{I}$ -LD78) and  $^{125}\text{I}$ -RANTES ( $^{125}\text{I}$ -CCL5), 873140 was an ineffectual antagonist of  $^{125}\text{I}$ -RANTES binding (but did block binding of  $^{125}\text{I}$ -MIP-1 $\alpha$  ). Furthermore, 873140 blocked the calcium response effects of CCR5 activation by CCL5 (RANTES) (as did the other antagonists) indicating a unique divergence of blockade of function and binding with this antagonist. The antagonism of CCR5 by 873140 is saturable and probe dependent consistent with an allosteric mechanism of action. The blockade of CCR5 by 873140 was extremely persistent with a rate constant for reversal of  $< 0.004 \text{ h}^{-1}$  ( $t_{1/2} > 136\text{h}$ ). Co-administration studies of 873140 with the four other allosteric antagonists yielded data that is consistent with the notion that all five of these antagonists bind to a common allosteric site on the CCR5 receptor. While these ligands may have a common binding site, they do not exert the same allosteric effect on the receptor as indicated by their differential effects on the

MOL 8685

binding of  $^{125}\text{I}$ -RANTES. This idea is discussed in terms of using these drugs sequentially to overcome HIV viral resistance in the clinic.

MOL 8685

## Introduction

### **The CCR5 Receptor-based mechanism of action of 873140, a potent allosteric non-competitive HIV entry-inhibitor**

With the discovery that the R5 strain of HIV utilizes the chemokine C CCR5 receptor for cell infection (Zhang and Moore, 1999; Shieh et al, 1998; Deng et al, 1996; Dragic et al, 1996; Alkhatib et al, 1996; Choe et al, 1996; Doranz et al, 1996) has come the opportunity for a completely new approach to preventing HIV infection, namely the blockade of CCR5 receptor interaction with the viral coat protein gp120. Subsequent reports of potent antagonists of CCR5-mediated HIV entry (Baba et al, 1999; Finke et al, 2001; Strizki et al, 2001; Kazmierski et al, 2003; Demarest et al, 2004a,b, Maeda et al, 2004) have validated this approach and have possibly opened a new era of AIDS therapy. There are data to support the notion that an allosteric mechanism is involved in the antagonism of HIV by low molecular weight antagonists of CCR5 (Kazmierski et al, 2002). The large size of the proteins involved in HIV fusion (i.e. CCR5, gp120) and the fact that mutational studies indicate that numerous regions of both CCR5 (Doranz et al, 1997; Rucker et al, 1996 Doms and Peiper, 1997; Lee et al, 1999 ; Picard et al, 1997; Atchison et al, 1996; Doranz et al, 1997) and gp120 (Kwong et al, 1998; Rizzuto et al, 1998; Smyth et al, 1998; Bieniasz et al, 1997; Ross et al, 1999) interact to promote HIV infection, suggest that low molecular weight antagonists of CCR5 preventing this process act through an allosteric mechanism (Kazmierski et al, 2002). In fact, an allosteric interaction between the HIV-1 envelope glycoprotein

MOL 8685

and the anti-HIV chemokine MIP-1 $\beta$  has been directly shown with kinetic binding studies (Staudinger et al, 2001). Consistent with this idea are data to indicate that there are separate binding loci on CCR5 for small antagonists such as Sch-C and the peptide chemokine RANTES (Tsamis et al, 2003; Wu et al, 1997; Blanpain et al, 2003). This present paper explores the mechanism of blockade of CCR5 receptors by a new potent antiviral 873140 (Demarest et al, 2004a,b; Maeda et al, 2004) and other CCR5 antagonists (see fig 1) and the relationship ship of this mechanism to therapeutic use and viral resistance.

## Materials and Methods

**CCR5 CHO Membrane Preparation** Chinese Hamster Ovary (CHO) cells stably expressing the human CCR5 receptor were grown in suspension with media containing 95% Excel 301 + 5% FBS + 4 mM L-glutamine + 250 ug/ml G418 (Invitrogen, Carlsbad, CA), harvested and pelleted by centrifugation. The weighed pellet was homogenized in 5 volumes of ice cold buffer containing 50 mM HEPES (Invitrogen, Carlsbad, CA) with protease inhibitors cocktail (2.5µg/ml Pefabloc, 0.1µg/ml Pepstatin A, 0.1µg/ml Leupeptin, 0.1µg/ml Aprotinin, Sigma, St. Louis, MO) at pH 7.4. The mixture was re-homogenized with a glass dounce for 10 to 20 strokes. Homogenate was centrifuged at 18,000 rpm in a F28/36 rotor using a Sorvall RC26. The supernatant was discarded and pellet re-suspended in 3 volumes of HEPES buffer. The pellet was homogenized and resuspended a total of three times. Finally, the pellet was reweighed, homogenized in 3X weight-to-volume HEPES buffer and aliquoted in 0.5 to 1.5 ml volumes into small vials for storage at -80°C. The protein concentration was determined using a BCA kit (Pierce, Rockford, IL).

**SPA Binding Studies.** Chinese Hamster Ovary (CHO) cells stably expressing the human CCR5 receptor were cultured in suspension, scaled up and membranes generated by a standard membrane preparation protocol. Ligand binding to CCR5 CHO membranes was measured using scintillation proximity assay (SPA). All test compounds were serially diluted in 100% DMSO at 100X of the final



MOL 8685

assay concentration. CCR5 receptor membranes (15µg/well) and WGA SPA beads (250µg/well Amersham, Piscataway, NJ) were diluted in assay buffer containing 50 mM HEPES pH 7.4 (Invotrogen, Carlsbad, CA), 1mM CaCl<sub>2</sub>, 5mM MgCl<sub>2</sub>, 1% BSA, 0.25 mg/ml bacitracin, 2.5µg/ml Pefabloc, 0.1µg/ml Pepstatin A, 0.1µg/ml Leupeptin, 0.1µg/ml Aprotinin and DMSO added to equal a final concentration of 2% per well (v/v) including compound/s (all buffer items from Sigma Aldrich, St. Louis, MO). The receptor/bead slurry was mixed in a 50 ml conical tube and preincubated for 1hr. at 4°C to allow the receptor/bead complex to form. Following preincubation, each well of a 96 well microtiter plate (Packard Optiplate 96 #6005190) received 1µl of test compound in 100% DMSO (final DMSO 2% v/v) or appropriate control, 50µls of receptor/bead mixture and 50µls of <sup>125</sup>I-MIP1α or <sup>125</sup>I-RANTES (Perkin Elmer, Boston, MA). Radioligand concentrations were typically 0.17nM (60,000CPM) for <sup>125</sup>I-MIP1α and 0.05nM (18,000CPM) for <sup>125</sup>I-RANTES unless otherwise noted. Plates were shaken at RT for 4hrs and binding signal was quantified on a Packard TopCount (30 s read).

Data reduction was performed using the Microsoft Excel Addins Robofit or Robosage (GlaxoSmithKline internal package). For concentration-response assays, the result of each test well was expressed as %B/Bo (% total specific binding); curves were generated by plotting the %B/Bo versus the concentration and the IC<sub>50</sub> derived using the equation:

$$Y = V_{\max} (1 - ([B]^n / ([B]^n + IC_{50}^n))) \quad \dots [1]$$

where  $K_B$  is the equilibrium dissociation constant of the (antagonist) ligand-receptor complex,  $V_{max}$  is the maximal degree of radioligand binding inhibition and  $IC_{50}$  the molar concentration of antagonist that blocks the binding by 50%. Plates were run for 14-point concentration-response curves in triplicate.

**Receptor Occupancy Offset Studies.** Offset experiments were run in 1.5 ml microcentrifuge tubes. Receptor/bead mixture (100 $\mu$ ls) was added to all assay tubes. Test compounds were introduced to each tube (1 $\mu$ l) at the appropriate time points (200X final concentration needed in 100% DMSO) and allowed to incubate at RT for 5hr. Tubes were washed by centrifugation (1000 RPM, 5min) and supernatant was aspirated. Fresh assay buffer (100 $\mu$ ls) was then added back to each tube. All tubes received equal washes either before or after compound addition to control for potential loss of signal due to repeated washing. Tubes were stored at 4°C overnight to maintain receptor integrity over the long experimental timeline. Once washes were complete, 50 $\mu$ ls of the compound/receptor/bead mixture from each tube was added to a 96 microtiter well. Reaction was initiated with the addition of 50 $\mu$ ls of 1.5nM or 0.2nM  $^{125}$ I-MIP1 $\alpha$ . Plates were shaken for two hours at RT and binding signal quantified on a Packard TopCount (30 sec read).

### **Functional Calcium Assay**

**BacMam Baculovirus Generation.** Recombinant BacMam baculoviruses for CCR5 (GenBank accession No. X91492) and the chimeric G-protein Gqi5 (Conklin et al., 1993) were constructed from pFASTBacMam shuttle plasmids using the

MOL 8685

bacterial cell-based Bac-to Bac system (Invitrogen, Carlsbad, CA) (Luckow et al., 1993). Viruses were propagated in Sf9 (*Spodoptera frugiperda*) cells cultured in Hink's TNM-FH insect media (JRH Biosciences, Lenexa, KS) supplemented with 10% fetal calf serum (Hyclone, Ogden, UT) and 0.1% (v/v) pluronic F-68 (Invitrogen, Carlsbad, CA) according to established protocols (O'Reilly et al., 1992).

**Cell Culture.** HEK-293 cells, stably transfected to express the human macrophage scavenging receptor (Class A, Type1; GenBank Accession No. D90187), were maintained in DMEM/F-12 media (1:1 mix) supplemented with 10% heat-inactivated fetal calf serum and 1.5µg/mL puromycin. The expression of this protein by the HEK-293 cells enhances their ability to stick to tissue culture-treated plasticware. All media, serum and supplements were from Invitrogen (Carlsbad, CA)

**Transduction of HEK-293 Cells.** HEK-293 cells were harvested using a non-enzymatic cell dissociation buffer (Invitrogen, Carlsbad, CA) and were subsequently resuspended in culture media supplemented with CCR5 and Gqi5 BacMam viruses (MOI of 50 and 12.5, respectively). The cells were plated at a density of 40,000 cells (100µl volume) per well in black 96 well clear bottom plates. The plates were incubated at 37°C, 5% CO<sub>2</sub>, 95% humidity for 24h to allow time for CCR5 and Gqi5 protein expression.

**Calcium Mobilization Experiments.** Growth media was removed from the transduced HEK-293 cells and they were washed once with FLIPR buffer

MOL 8685

(Calcium Plus assay kit dye reagent (Molecular Devices, Sunnyvale, CA) dissolved in DMEM/F-12 media containing 2.5 mM probenid and 0.1% bovine serum albumin (w/v)). 50µl of this dye solution, was then added to each well and the plates were incubated for 1h at 37°C, under 5% CO<sub>2</sub> and 95% humidity. The effects of various ligands on intracellular calcium levels were examined using FLIPR (Molecular Devices, Sunnyvale, CA).

### Statistical Analysis of significance of regression

The relationship between variables was quantified by a t-value calculated as:

$$t = r \cdot \sqrt{\frac{(n-2)}{(1-r^2)}} \quad , \quad \text{d.f.} = n-2 \quad \dots[2]$$

where

$$r = \frac{s_{xy}}{\sqrt{s_x^2 s_y^2}} \quad \dots[3]$$

and

$$s_{xy} = \sum xy_i - \frac{(\sum x_i)(\sum y_i)}{n_i} \quad \dots[4]$$

$$s_x^2 = \sum x_i^2 - \frac{(\sum x)^2}{n_i} \quad \dots[5]$$

and

$$s_y^2 = \sum y_i^2 - \frac{(\sum y)^2}{n_i} \quad \dots[6]$$

## Kinetics of Offset

Data were fit to a first order receptor offset model of the form:

$$\rho_t = \rho_e e^{-kt} \quad \dots[7]$$

where  $\rho_e$  is the fractional receptor occupancy by the antagonist at equilibrium,  $k$  is the rate of offset,  $t$  is time and  $\rho_t$  is the fractional antagonist receptor occupancy at time  $t$ . The values for  $\rho_e$  and  $\rho_t$  were obtained from mass action:

$$\rho = \frac{[B]/K_B}{[B]/K_B + 1} \quad \dots[8]$$

where  $[B]$  is the antagonist concentration and  $K_B$  the equilibrium dissociation constant of the antagonist-receptor complex. Values of  $[B_e]/K_B$  and  $[B_t]/K_B$  were obtained by fitting the values for radioligand binding in the absence and presence of the antagonist to the  $^{125}\text{I}$ -MIP-1 $\alpha$  saturation curve to the model for simple competitive antagonism for MIP-1 $\alpha$ :

$$\rho = \frac{[^{125}\text{I-MIP-1}\alpha / K_d] B_{\max}}{[^{125}\text{I-MIP-1}\alpha / K_d] + [B]/K_B + 1} \quad \dots[9]$$

and for non-competitive antagonists:

$$\rho = \frac{[^{125}\text{I-MIP-1}\alpha / K_d] B_{\max}}{[^{125}\text{I-MIP-1}\alpha / K_d] ([B]/K_B + 1) + [B]/K_B + 1} \quad \dots[10]$$

A regression of  $\ln(\rho_t/\rho_e)$  vs time yields a straight line of slope =  $k$ .

MOL 8685

## Drugs and Materials

1 M HEPES, pH 7.4, Gibco, Cat. No. 15360-080, Bacitracin, Sigma Catalog Number. B-0125, Bovine Serum Albumin, Sigma, Cat. No. A-7888, MgCl<sub>2</sub>, J.T. Baker 2444-01, CaCl<sub>2</sub>, Sigma, Cat. No. C5080, MIP1 $\alpha$ , Peprotech, Cat. No. 300-08, Sigmacote, Sigma, Cat. No. SL2, Scintillation Proximity Beads, Wheat Germ, Agglutinin, Amersham, Cat No. RPNQ 0001, [<sup>125</sup>I]MIP1 $\alpha$ , NEN (#NEX298), Packard 96 well flat-bottom Optiplate, Cat. No. 6005190, Falcon 96 well round-bottom plate, Cat. No. 3077, TOPSEAL-S, Packard, Cat. No. 6005161, Dimethyl Sulfoxide, EM Science, Cat. No. MX1458-6, Siliconized Pipette tips, Accutip, volume 200-1300uL, Cat. No. P5048-85, Siliconized Pipette tips, Bio Plas, Inc., volume 1-200uL, Cat. No. 60828-908, Reagent Reservoir, Elkay, Cat. No. 175-RBAS-000

RANTES and MIP-1 $\alpha$  peptides were obtained from PeproTech Inc., Rocky Hill, NJ), SchC, (Z)-(4-bromophenyl){1'-[(2,4-dimethyl-1-oxido-3-pyridinyl)carbonyl]-4'-methyl-1,4'-bipiperidin-4-yl}methanone O-ethyloxime was synthesized using procedures analogous to these disclosed in the literature (Palani et al, 2001; Baroudy et al, 2000a). SchD, 4,6-dimethyl-5-[[4-methyl-4-((3S)-3-methyl-4-((1R)-2-(methyloxy)-1-[4-(trifluoromethyl)phenyl]ethyl)-1-piperazinyl)-1-piperidinyl]carbonyl]pyrimidine (Tagat et al, 2004) was synthesized using procedures analogous to these disclosed in the literature (Baroudy et al, 2000b). UK-427,857 (4,4-difluoro-N-((1S)-3-((3-endo)-3-[3-methyl-5-(1-methylethyl)-4H-1,2,4-triazol-4-yl]-8-azabicyclo[3.2.1]oct-8-yl})-1-

MOL 8685

phenylpropyl)cyclohexanecarboxamide) was synthesized using procedures analogous to these disclosed in the literature (Perros et al, 2001).

## Results

### Receptor Models used in Analysis

The estimation of antagonist potencies and kinetics requires comparison of data to quantitative models of receptor function (see Appendix A of supplemental material). Specifically, the standard Ehlert (1988) model is described whereby the tracer ligand (either radioligand or functional agonist) can concomitantly bind to the receptor with the antagonist; this model predicts parallel shifts to the right of the saturation curve for a radioligand when the allosteric antagonist is present (see fig 2A). A variant of this model is described that allows allosteric ligands to not affect the binding of agonists and radioligands but to prevent activation of the receptor by agonists. Specifically, the Ehlert model predicts non-competitive blockade of function but not binding if it is assumed that binding of the antagonist precludes receptor activation- see Fig 2B). Another model is described whereby the binding of the antagonist precludes binding of the tracer ligand in a non-competitive manner (denoted 'non-competitive' allosteric model)(described in Appendix B of supplemental material); this model predicts depression of the maxima of saturation binding curves with no concomitant dextral displacement. This model is required to describe the observed binding characteristics of these antagonists.

Two antagonist binding models (referred to as three-ligand models) also are presented to describe possible interactions between the allosteric ligands as



MOL 8685

they bind to the receptor (Appendix 1). Finally, a new model of allosteric function presented by Hall (2000) is described as another option to account for the different characteristics of 873140 blockade of the functional effects of RANTES but not  $^{125}\text{I}$ -RANTES binding (denoted ‘Hall functional allosteric model’-see Appendix C of supplemental material).

### **Binding of $^{125}\text{I}$ -MIP-1 $\alpha$**

Saturable binding of  $^{125}\text{I}$ -MIP-1 $\alpha$  was obtained using a scintillation proximity assay (SPA). The equilibrium dissociation of  $^{125}\text{I}$ -MIP-1 $\alpha$  was  $0.56 \text{ nM} \pm 0.08 \text{ nM}$  (95% c.l. 3.8 pM to 0.82 nM) with a maximal receptor binding of 120 fmoles/mg protein. Non radioactive MIP-1 $\alpha$  produced displacement of  $^{125}\text{I}$ -MIP-1 $\alpha$  (see fig 3A) in an apparently competitive manner (see fig 3B). The  $\text{IC}_{50}$  for half-maximal inhibition of binding varied with concentration of radiolabel (as expected for competitive antagonism)- see fig 3C according to the Cheng-Prusoff (1973) correction:

$$K_B = \text{IC}_{50} / (1 + [A^*]/K_d) \quad \dots[11]$$

where  $[A^*]$  is the concentration of  $^{125}\text{I}$ -MIP-1 $\alpha$ ,  $K_d$  the equilibrium dissociation constant of the  $^{125}\text{I}$ -MIP-1 $\alpha$  /receptor complex and  $\text{IC}_{50}$  the molar concentration of MIP-1 $\alpha$  producing 50% inhibition of blockade. A regression of  $\text{IC}_{50}$  values on concentration of radioligand (according to equation 11) yielded a linear regression (see fig 3C).

The radioligand  $^{125}\text{I}$ -MIP-1 $\alpha$  was displaced by TAK779 as well but, in this case, the effects appeared to be of a non-competitive nature (see fig 4A,B). The

MOL 8685

IC<sub>50</sub> values did not change with elevations of the concentration of radioactive label as shown in fig 5. This is indicative of non-competitive antagonism whereby the magnitude of the IC<sub>50</sub> value is independent of the concentration of radioligand and also is an estimate of the K<sub>B</sub>, the equilibrium dissociation constant of the antagonist-receptor complex (see Appendix B in supplementary material and Kenakin, 2004a for further details). The mean pK<sub>B</sub> (-log K<sub>B</sub>) for this antagonist is  $7.8 \pm 0.14$  (95 % c.l. = 8.1 to 7.5). A similar pattern was observed for Sch-C (SCH 351125) with non-competitive antagonism of <sup>125</sup>I-MIP-1α binding (see fig 4C,D) and a pK<sub>B</sub> of  $8.2 \pm 0.1$  (95 % c.l. = 8.4 to 8.0). Sch-D (SCH 417,690) also produced non-competitive antagonism of <sup>125</sup>I-MIP-1α binding (see fig 4E,F) with a pK<sub>B</sub> of  $8.4 \pm 0.1$  (95 % c.l. = 8.2 to 8.6). The same pattern was observed for UK-427,857 (non-competitive antagonism of <sup>125</sup>I-MIP-1α binding -see fig 3G,H) with a pK<sub>B</sub> of  $8.7 \pm 0.08$  (95 % c.l. = 8.5 to 8.9). For all four non-competitive antagonists, the magnitude of the IC<sub>50</sub> was not affected by the concentration of the radioligand (Fig 5). 873140 produced non-competitive antagonism of <sup>125</sup>I-MIP-1α binding (see fig 6A,B) with the IC<sub>50</sub> demonstrating no effect of radioligand concentration on IC<sub>50</sub> as well (see fig 6C). The mean value for the pK<sub>B</sub> was  $8.6 \pm 0.07$  (95 % c.l. = 8.5 to 8.8). These data are summarized in Table 1.

### **Binding of <sup>125</sup>I-RANTES**

Experiments were conducted to determine the potency of the antagonists as displacers of <sup>125</sup>I-RANTES. As seen in fig 7A, displacement was produced by Sch-D, TAK779, UK-427,857 and to a very much lesser extent, 873140. Of note is

MOL 8685

the fact that the maximal displacement by each antagonist varied. A two-way analysis of variance ordering the maximal displacement produced by each antagonist as replicate sample rows vs separate antagonists as columns indicates that there is no significant variation between replicate readings for each antagonist (four separate samples measured,  $F=0.69$ ,  $df=3,9$ ) but a highly significant difference between antagonist type ( $F=78.2$ ,  $df=3,9$ ,  $p<0.0001$ ). These data confirm an earlier report of the same phenomenon by Maeda et al (2004). The fact that a submaximal displacement (13%) was obtained for 873140 (as compared to an nsb determined with Sch-C) is consistent with receptor system behavior according to the Ehlert model and not the non-competitive model. Moreover, the differences in the maximal displacements indicate an allosteric mechanism and differing values of cooperativity constant  $\alpha$  for the antagonists for RANTES interaction with CCR5.

The minimal effect of 873140 on  $^{125}\text{I}$ -RANTES binding indicates a very weak effect of this antagonist on RANTES binding. An estimate of the quantitative difference between the allosteric effects of 873140 and the other antagonists, for example Sch-D, was made by projecting saturation curves for RANTES in the absence and presence of the antagonists. Fig 7B shows the specific binding of  $^{125}\text{I}$ -RANTES and the maximal displacement of the binding of 40 pM  $^{125}\text{I}$ -RANTES produced by 873140 and Sch-D as putative points on the allosterically shifted saturation curve in the presence of a high concentration of antagonist ( $[\text{B}]/K_B \geq 300$ )- see Ehlert model, fig 1A. It can be seen that the effects

MOL 8685

of 873140 are minimal with an estimated  $\alpha$  value for RANTES with this antagonist of 0.8. In contrast, the estimated minimal value for Sch-D from these data is  $\alpha=0.06$  and it should be noted that, since specific binding was reduced to noise levels, the shift in the curve could be substantially greater. Therefore, 0.06 is the upper limit for the cooperativity constant for Sch-D and  $^{125}\text{I}$ -RANTES ( $\alpha \leq 0.06$ ). The fact that the  $\alpha$  value for 873140 is at least 13-fold greater than Sch-D with  $^{125}\text{I}$ -RANTES as the receptor probe indicates that different allosteric conformations are made by these antagonists (Christopoulos and Kenakin, 2002).

### Kinetics of Recovery from Blockade

The effect of washing with drug free media was explored in the  $^{125}\text{I}$ -MIP-1 $\alpha$  binding assay. Fig 8A shows the reversal from blockade of a single concentration of  $^{125}\text{I}$ -MIP-1 $\alpha$  by non-radioactive MIP-1 $\alpha$ , Sch-C, TAK779 and 873140. As can be seen from this figure, washing over a period of 4 hours at room temperature caused reversal of the binding by MIP-1 $\alpha$  but not the allosteric antagonists. Fig 8B shows data from a differently designed experiment, namely a much longer wash period (51 h). To preserve the viability of the receptor preparation, these studies were conducted at 4° C. The dependence of antagonist occupancy on time was assessed by subjecting the data to a t test for the significance of a relationship between two variables (time and occupancy) –see methods. The value of t for the regression of ln receptor occupancy vs time showed that there was a significant effect of time on the occupancy for TAK779, Sch-C, Sch-D, MIP-

1 $\alpha$  and UK427,857 (see Table 2). In contrast, no significant relationship between the receptor occupancy of 873140 and time was observed ( $p < 0.05$ ) indicating that this antagonist did not appreciably dissociate from the receptor over the 51 h wash period. The rates of offset for the antagonists are given in Table 2.

### Functional Studies

The effect of the allosteric antagonists on calcium fluorescence responses to RANTES in HEK 293 cells transfected with CCR5 receptor were measured. As shown in fig 9A to D, TAK 779, Sch-C, Sch-D and UK427857 produced concentration dependent non-competitive antagonism of RANTES responses. These data were consistent with the effects of these antagonists on RANTES binding. Also consistent with the binding studies, 873140 produced blockade of calcium responses to MIP-1 $\alpha$  (fig 9F). However, interestingly, 873140 also produced concentration dependent non-competitive antagonism of responses to RANTES (fig 9E) in stark contrast to the lack of effect of this antagonist on RANTES binding.

The depression of dose-response curves to RANTES by 873140 with no concomitant effect on binding can be predicted, under certain circumstances, by one version of the Ehlert model. Specifically, if it is assumed that the allosteric modulator does not affect the binding of the agonist (or radioligand) but does prevent receptor activation by the agonist, then the effects observed for 873140 on RANTES binding and function can be accounted for. In this variant of the Ehlert model, only the [AR] species (receptor bound to agonist without the

MOL 8685

allosteric modulator present) produces response. On a molecular level, this can occur if the allosteric modulator produces a conformational change in the receptor that does not interact with G-protein (fig 2B). The lack of effect on binding would be produced by a value for  $\alpha$  near unity. This is consistent with the estimated value of  $\alpha=0.8$  found for 873140 and  $^{125}\text{I}$ -RANTES binding.

This effect also can be described with a new a functional model of allosterism described by Hall (2000). This model, described in Appendix C (supplementary material), indicates that receptor binding assays and receptor functional assays monitor changes in different receptor species. Therefore, a modulator that promotes radioligand binding to non-activated receptor species while preventing the transition to activated receptor species will not affect binding but block function. An example of the use of this model to calculate the absence of significant effects on binding but a depression of function is given in Appendix C (supplementary material). The important aspect of this simulation is the fact that the same antagonist (constant values of  $\epsilon$  and  $\phi$ ) can produce this effect for one agonist (defined value of  $\chi$ ) but not another; this is consistent with the effects of 873140 with the different ligands MIP-1 $\alpha$  and RANTES.

### **Allosteric Antagonist-Interactions**

The possible interactions of 873140 and the other antagonists were explored by measuring the potency of 873140 (denoted as the reference antagonist) as a displacer of  $^{125}\text{I}$ -MIP-1 $\alpha$  in the absence and presence of a range of concentrations of each of the other antagonists (denoted the test antagonist).

MOL 8685

The presence of the test antagonist produces a diminution of the binding window for  $^{125}\text{I}$ -MIP-1 $\alpha$  therefore only an approximate 10-fold range of concentration can be used to determine the displacement curve of the reference antagonist. A plot of the observed  $\text{IC}_{50}$  values for the test antagonist in the presence of a range of concentrations of the reference antagonist vs the initial  $B_0$  values of the  $^{125}\text{I}$ -MIP-1 $\alpha$  binding can be predicted from the non-competitive allosteric model according to the following relationship (see Appendix 1):

$$\frac{B'_0}{B_0} = \frac{K_A}{\text{IC}_{50} (1 - \alpha)} + \frac{\alpha}{(1 - \alpha)} \dots [12]$$

where  $\text{IC}_{50}$  refers to the potency of the reference antagonist (molar concentration producing 50% displacement of the radioligand) in the presence of the test antagonist,  $K_A$  is the equilibrium dissociation constant of the reference antagonist-receptor complex (also the  $\text{IC}_{50}$  value for the reference antagonist in the absence of test antagonist for non-competitive antagonism), and  $\alpha$  is the cooperativity factor describing the interaction between the reference and test antagonist through the protein. The ratio  $B'_0/B_0$  depicts the fractional decrease in basal binding produced by the test antagonist.

Various patterns for this relationship are predicted that are dependent upon whether or not the two allosteric modulators can interact (i.e. whether the binding of one allosteric modulator affects the binding of the other); these patterns are given by equation 12, (see Appendix 1); Fig 10 shows a double

logarithmic representation of this relationship under a variety of conditions. If  $\alpha > 1$ , the convex regression to the left reflects the fact that the binding of one allosteric modulator increases the affinity of the receptor for the other allosteric modulator. A linear vertical line indicates the condition whereby  $\alpha = 1$ , namely a case of completely independent binding of the two modulators. This denotes a case where the allosteric modulators bind to their own sites on the receptor and do not affect each other, only the binding of the tracer (in this case  $^{125}\text{I}$ -MIP-1 $\alpha$ ). A convex regression to the right denotes a case whereby the binding of one allosteric modulator negatively impacts the binding of the other ( $\alpha < 1$ ). A linear regression with negative slope indicates a case for  $\alpha = 0$  whereby the two allosteric modulators exhibit prohibitive binding. Thus, when one antagonist is bound, the affinity of the receptor for the other diminishes to very low values. The most simple case of prohibitive binding is where the antagonists bind to the same site on the receptor. It can be seen that this is predicted by the special case for equation 12 when  $\alpha = 0$  (see Appendix 1):

$$\text{Log } (B'_0/B_0) = -\text{Log } (IC_{50}/K_A) \dots [13]$$

It should be noted that, even in this scenario, the allosteric perturbation of the modulators on the receptor affecting the binding of the tracer, is unique to that modulator, i.e. the effect on the tracer (either  $^{125}\text{I}$ -MIP-1 $\alpha$  or HIV) depends on which antagonist binds to the site. Thus, there is still allosteric texture of antagonism even if the modulators share the same allosteric binding site.



Fig 11A shows displacement curves for 873140 in the absence and presence of a range of concentrations of TAK779. It can be seen that the presence of TAK 779 reduced the binding window for the displacement curves but did not produce much significant change in the  $IC_{50}$  of 873140. Fig 11B shows a regression of the log of the depression in  $B_0$  produced by the test antagonist TAK 779 upon the log of the ratio of the  $IC_{50}$  values for 873140 in the presence and absence of TAK 779 (according to equation 12, see also Appendix 1). It can be seen that a linear relationship with a slope of  $-1.1$  resulted (see Table 3 for quantitative data). The 95% confidence limits of the slope contain unity therefore these data are consistent with the model defined when  $\alpha=0$  for interaction between the two antagonists (consistent with prohibitive binding and a common binding site for the two antagonists). Fig 11C and 11D show the same data for Sch-C. It can be seen from the data in Table 3 that a common binding site ( $\alpha=0$ ) is indicated for 873140 and Sch-C as well. Identical qualitative results were obtained from co-administration studies with Sch-D (fig -11E,F; data Table 3) and UK 427,857 (Fig 11G,H and Table 3).

## Discussion

The data described in this paper are discussed in terms of an allosteric interaction between the antagonists and the chemokine radioligands. As reviewed in the introduction, the size of the proteins involved and the breadth of interaction between them, would predict that steric hindrance involving the small molecule antagonists and the proteins are insufficient to account for the blockade of the protein-protein interaction. Chemokine receptors are known to function allosterically with ligands as shown in the direct kinetic binding studies between the chemokine MIP-1 $\beta$  and HIV envelope glycoprotein (Staudinger et al, 2001). Similarly, data from other studies implicate allosterism as a mode of action for chemokine receptors. For example, incomplete displacement of receptor radioactive peptide ligand  $^{125}\text{I}$ -MIP-1 $\alpha$ , a hallmark of allosteric interaction, has been observed for chemokine CCR1 receptors by the allosteric small molecule modulator UCB35625 (Sabroe et al, 2000). Similarly, different maximal displacement of chemokine  $^{125}\text{I}$ -I-TAC (interferon-inducible T cell  $\alpha$  chemoattractant) by the chemokine agonists IP-10 (10-kDa interferon-inducible protein) and MIG (monokine induced by human interferon- $\gamma$ ) has been observed for CXCR3 receptors (Cox et al, 2001). Antibodies also have been used to discern differences in the effects of allosteric ligands. Thus, the antibody a-hCXCR3 blocks the agonist effects of IP-10 but not those of ITAC (Cox et al, 2001). Similarly, the CCR5 receptor antibody MC-1, while it does not induce but rather blocks chemokine response and blocks binding of chemokine to CCR5, actively

MOL 8685

promotes receptor internalization, a behavior usually associated with receptor activation (Blanpain et al, 2002). Finally, separate binding domains have been suggested for the small molecule antagonist Sch-C and the chemokine RANTES (Tsamis et al, 2003; Wu et al, 1997; Blanpain et al, 2003) consistent with an allosteric interaction between these ligands through the receptor.

While these data are all consistent with the notion that CCR5 and these ligands are allosteric antagonists of CCR5. In this study, it is the probe dependence and saturability of the antagonism of CCR5 by 873140 that strongly suggest an allosteric mode of action (Kenakin, 2004b). The most direct and compelling reason for suggesting that 873140 and the other antagonists interact with CCR5 in an allosteric fashion are the differences in binding seen with  $^{125}\text{I}$ -MIP-1 $\alpha$  and  $^{125}\text{I}$ -RANTES and the concomitant striking difference between the effects on RANTES binding and function. For antagonists with an orthosteric mode of action (steric occlusion of the tracer binding site), all 'blocked' receptors can be assumed to be equal, i.e the nature of the antagonist is immaterial since the result on the receptor is the same. In allosteric terms, 'blocked' receptors (by the antagonist) cannot be assumed to be equal since the allosteric antagonist produces a change in conformation and, as quantified by the magnitude of the cooperativity constant  $\alpha$ , different allosteric modulators may produce different conformations of the receptor. Thus, a 'blocked' receptor simply becomes a changed receptor with its own set of affinities for various tracers (Kenakin, 2004b). In the case of 873140, the allosterically modulated receptor does not allow

MOL 8685

binding of  $^{125}\text{I}$ -MIP-1 $\alpha$  but does allow  $^{125}\text{I}$ -RANTES to bind, albeit in a functionally ineffective manner. Also, allosteric texture in the antagonism by other allosteric modulators such as Sch-C and TAK779 is demonstrated by the difference in the maximal displacement of  $^{125}\text{I}$ -RANTES (see fig 9) . While inconsistent with orthosteric antagonism this is completely consistent with an allosteric mode of action since allosteric modulation is probe dependent, i.e. an allosteric conformational change that is catastrophic for one receptor probe may be inconsequential to another. Blockade of  $^{125}\text{I}$ -MIP-1 $\alpha$  binding but not  $^{125}\text{I}$ -RANTES binding agrees with this profile of behavior.

While sigmoidal displacement curve for  $^{125}\text{I}$ -MIP-1 $\alpha$  for the CCR5 antagonists were produced, this cannot be taken as evidence for competitive binding. In radioligand binding experiments, such curves also can result from allosteric and/or non-competitive antagonism. An inspection of the relationship between the concentrations of radioligand bound and antagonist show a depression of the maximal binding indicative of non-competitive antagonism. The relative geography of radioligand tracer and antagonist cannot be inferred from the displacement curves, i.e. whether or not the antagonist occupies the same binding site as does  $^{125}\text{I}$ -MIP-1 $\alpha$ . The verisimilitude of the  $^{125}\text{I}$ -RANTES binding to the prediction of the Ehlert model (1988) (whereby a ternary species binding both  $^{125}\text{I}$ -RANTES and 873140) suggests that an allosteric mechanism with separate binding sites for the antagonist and radioligand with concomitant effects transmitted through the protein is operable. In fact, Maeda and colleagues

MOL 8685

(2004) have shown the existence of such a ternary species (both radioactive RANTES and 873140 bound to the receptor simultaneously) with radiolabelled RANTES and 873140. The non-competitive allosteric effects of 873140 as well as the other CCR5 antagonists tested in these experiments resemble the activity of the endogenous serotonin receptor tetrapeptide allosteric modulator 5-HT moduline which reduces the maximal binding and response of serotonin for 5-HT<sub>1B</sub> receptors (Fillion et al, 1996; Massot et al, 1996).

A complicated pattern of behavior is demonstrated by 873140 in the lack of binding effect for <sup>125</sup>I-RANTES but blockade of RANTES function. In this case, 873140 allows RANTES to bind but not activate G-protein to elicit response. The variant of the Ehlert model whereby response is produced only by agonist-occupied receptor (with no allosteric modulator present) predicts non-competitive antagonism of agonist effect but no effect on the same agonist binding (as a radioligand species) if  $\alpha$  is near unity. This effect also can be described in molecular terms with a recently described allosteric function model by Hall (2000-see Appendix C supplementary material). In this model, receptor activation is separated from ligand binding (as in standard two-state and ternary complex models); this allows the allosteric ligand to affect activation and binding separately. In terms of this model, the key to understanding the divergence of binding and functional effects is to consider the different array of receptor species quantified by each assay. Thus, the radioligand bound species [AR<sub>i</sub>], [AR<sub>a</sub>], [ABR<sub>i</sub>] and [ABR<sub>a</sub>] are measured for binding while for function, only the

MOL 8685

activated  $[R_a]$  species are observed (namely  $[R_a]$ ,  $[AR_a]$ ,  $[BR_a]$  and  $[ABR_a]$ ). This can lead to conditions where no effect can be seen on radioligand bound species in the face of non-competitive diminution of receptor function. As seen in Appendix C (supplementary material), this can be modeled with an appropriate  $\epsilon < 1$  with concomitant  $\phi > 1$  for the antagonist, i.e. the allosteric modulator selectively binds to the inactive state of the receptor and also promotes agonist binding to the receptor. Lack of allosteric effect on binding but not function has been reported for other receptors. For example, 7-hydroxyiminocyclopropan[b]chromen-1a-carboxylic acid ester (CPCCOEt) is a potent non-competitive antagonist of glutamate receptor response but also is a completely ineffective displacer of glutamate binding (Litschig et al, 1999). It should be noted that the G-protein milieu surrounding the receptor is different in the binding vs functional experiments. Specifically, the FLIPR experiments mediated a chimeric G-protein response opening the possibility that 873140 blocks the interaction of the receptor with the chimeric G-protein but not the natural G-protein. This possibility is made less likely by the finding of Maeda et al (2004) showed that 873140 blocks the chemotactic effects of RANTES in MOLT4 cells (Maeda et al, 2004). It should also be noted that for the Hall model to be operative (i.e.  $\epsilon < 1$ ), this would suggest that 873140 would demonstrate inverse agonist properties in constitutively active receptor systems. Presently it is not known if 873140 is an inverse agonist.

The co-administration studies are consistent with the idea that 873140 and the other antagonists bind to a common allosteric binding site on the receptor (i.e.  $\alpha$  for the co-administration model  $\rightarrow 0$ ). This should not be interpreted to suggest that these antagonists have the same effect on the receptor to achieve prevention of HIV entry. This latter property is controlled by the co-operativity factors for HIV, not other antagonists i.e. each antagonist prevents HIV fusion by inducing its' own effect on the receptor. This idea is underscored by the differences in the binding of with  $^{125}\text{I}$ -MIP-1 $\alpha$  and  $^{125}\text{I}$ -RANTES produced by the various antagonists, i.e. while Sch-C blocks both  $^{125}\text{I}$ -MIP-1 $\alpha$  and  $^{125}\text{I}$ -RANTES, 873140 only blocks the binding of  $^{125}\text{I}$ -MIP-1 $\alpha$ .

There are therapeutic implications of an allosteric mechanism that pertain to the use of these antagonists in the treatment of HIV. Chronic treatment with a CCR5 antagonist might select for gp120 variants able to infect cells via binding to allosterically modified receptor. HIV-1 is known to mutate resulting in sequence changes in its Env complex with no concomitant loss of function (Wyatt and Sodrowski, 1998; Poignard et al, 2001). Passage studies with AD101, an antagonist structurally-related to Sch-C, have indicated that resistance can occur through the production of an escape mutant in the presence of antagonist (Trkola et al, 2002; Kuhmann et al, 2004). If another allosteric antagonist induces a different conformation, then it is possible that the mutant virus would not be cross resistant to both drugs. It is interesting to note that mutation studies on the Sch-C analog AD101-resistant escape mutant virus CC101.19 indicate that the

MOL 8685

four amino acid substitutions on the V3 loop of gp120 require the native three-dimensional presentation to the receptor to confer resistance (Kuhmann et al, 2004); this would suggest that allosteric conformational changes may be effective in disrupting the tertiary interaction of the gp-120 and CCR5 interfaces. This would offer a treatment option following the emergence of resistance to the first agent. With regard to 873140, this idea is supported directly by a recent report by Maeda et al (2004) who show that 873140 produces a different profile for antibody binding to CCR5 than does Sch-C or TAK-779. Similarly, the COC101.19 escape mutant virus, while being insensitive to the small molecule AD101, is sensitive to the chemokine RANTES (Kuhmann et al, 2004). These data suggest that the conformation produced by AD101 differs from that made by RANTES (an agonist that promotes coupling of G-proteins to CCR5). This is consistent with the notion that different CCR5 conformations will present problematic receptor conformations to resistant viruses.

The offset experiments showed a difference between the rate of offset of the non-competitive antagonists and the peptide chemokine MIP-1 $\alpha$ . No offset of the non-competitive antagonists was observed at room temperature for 5 h precluding direct comparison to MIP-1 $\alpha$ . However, an internal comparison of the non-competitive antagonists was done under identical conditions; the comparison of the mean rates and 95% confidence limits of the estimates indicated three general groups. The antagonists with the most rapid offset were Sch-C and TAK779. A statistically slower set of offset rates was obtained for Sch-



MOL 8685

D and UK427,857. Finally, no significant offset over the 51 h time period was observed for 874140. It is not possible to determine a half time for reversal of receptor antagonism for 873140 from these data since the statistical significance of time dependence depends both upon the slope of the offset line and the scatter in the data. Under these conditions, a measurable offset for 873140 would need to be determined under these experimental circumstances for a half time to be calculated. However, what can be done is an estimation of the lower limit of the half-time from the measured offset of UK 427,857. The data in fig 8 indicate that the half time for reversal of UK 427,857 antagonism of CCR5 is 136 h. Since the offset of 873140 is measurably slower than that obtained for UK 427,857 under these experimental conditions, it can be estimated that the half time for reversal of 873140 is  $> 136$  h. It would be predicted that protection from HIV infection requires constant allosteric modulation of the receptor, therefore the particularly persistent antagonism of CCR5 by 873140 suggests that this ligand may have a therapeutic advantage over more labile (higher rate of offset from the receptor) antagonists. In view of the inordinately slow offset from the receptor ( $<0.004$  h<sup>-1</sup>), after exposure to 873140, infectability may depend more on the generation of new CCR5 receptors on the cell surface than on offset of 873140.

In general, 873140 demonstrates characteristics of CCR5 receptor blockade similar to other CCR5 antagonists found to reduce HIV viral load in humans. In addition, the fact that this is an allosteric ligand that produces a receptor conformation different from that produced by other antagonists, suggests that

MOL 8685

this ligand may yield a unique viral resistance profile. It will be interesting to see if the unusually slow offset of 873140 from the receptor will translate into a unique therapeutic profile for this molecule.

MOL 8685

## **Acknowledgements**

We wish to thank Cecilia Koble, Neil Bifulco, Virgil Styles for synthesizing Sch-C, Sch-D and UK 427,857. We also wish to thank Larry Boone (Dept of Virology) for very useful input into this manuscript.

MOL 8685

## References

- Alkhatib G, Combadiere C, Broder CC, Feng Y, Kennedy PE, Murphy PM, and Berger EA (1996) CC CKR5: A RANTES, MIP-1, MIP-1 receptor as a fusion cofactor for macrophage-tropic HIV-1. *Science* **272**:1955-1958.
- Atchison RE, Gosling J, Monteclaro FS, Franci C, Digilio L, Charo IF and Goldsmith M (1996) Multiple extracellular elements of CCR5 and HIV-1 entry: Dissociation from response to chemokines *Science* **274**: 1924-1926.
- Baba M, Nishimura O, Kanzaki N, Okamoto M, Sawad H, Iizawa Y, Shiraishi M, Aramaki Y, Okonogi K, Ogawa Y, *et. al.*(1999) A small-molecule, nonpeptide CCR5 antagonist with highly potent and selective anti-HIV-1 activity *Proc. Natl. Acad. Sci. USA* **96**: 5698-5703.
- Baroudy B, Clader, JW, Josien HB, McCombie SW, McKittrick BA, Miller MW, Neustadt BR, Palani A, Steensma R, Tagat JR, *et. al.* (2000) PCT Int. Appl. WO 2000066559
- Baroudy BM, Clader, JW, Josien HB, McCombie SW, McKittrick BA, Miller MW, Neustadt BR, Palani A, Smith EM, Steensma R, *et. al.* (2000) PCT Int. Appl. , WO 2000066558
- Bieniasz PD, Fridell RA, Aramori I, Ferguson SS, Caron MG, and Cullen BR (1997) Multiple Active States and Oligomerization of CCR5 Revealed by Functional Properties of Monoclonal Antibodies *EMBO J* **16**: 2599-2609.

MOL 8685

- Blanpain C, Vanderwinden J-M, Cihak J, Wittamer V, Le Poul E, Issafras H, Strangassinger M, Vassart G, Marullo S, Schlondorff D, *et. al.* (2002) Multiple active states and oligermization of CCR5 revealed by functional properties of monoclonal antibodies. *Mol. Biol. Cell* **13**:723-737.
- Blanpain C, Doranz BJ, Bondue A, Govaerts C, De Leener A, Vassart G, Doms RW, Proudfoot A, and Parmentier M. (2003) The core domain of chemokines binds CCR5 extracellular domains while their amino terminus interacts with the transmembrane helix bundle. *J Biol Chem* **278**:5179-5187.
- Cheng, Y.C., and Prusoff, W.H. (1973). Relationship between the inhibition constant (K<sub>i</sub>) and the concentration of inhibitor which causes 50 percent inhibition (I<sub>50</sub>) of an enzymatic reaction. *Biochem.Pharmacol.* , **22**, 3099-3108.
- Choe, H., Farzan, M., Sun, Y., Sullivan, N., Rollins, B., Ponath, P.D., Wu, L., MacKay, C.R., LaRosa, G., Newman, G., Gerard, W., Gerard, N., and Sodroski, J. (1996) The  $\beta$ -chemokine receptors CCR3 and CCR5 facilitate infection by primary HIV-1 isolates. *Cell* **85**:1135-1148.
- Christopolous A, and Kenakin TP (2002) G-protein coupled receptor allosterism and complexing. *Pharmacol. Rev.* **54**: 323-374.
- Conklin BR, Farfel Z, Lustig KD, Julius D and Bourne HR (1993) Substitution of three amino acids switches receptor specificity of Gq  $\alpha$  to that of Gi  $\alpha$ . *Nature (Lond)* **363**:274-276.
- Cox MA, Jenh C-H, Gonsiorek W, Fine J, Narula SK, Zavodny PJ and Hipkin RW. (2001) Human interferon-inducible 10-kDa protein and human

- interferon-inducible T cell  $\alpha$  chemoattractant are allotropic ligands for human CXCR3: Differential binding to receptor states. *Mol Pharmacol* **59**: 707-715.
- Demarest,J, K. Adkison, S. Sparks, A. Shachoy-Clark, K. Schell, S. Reddy, L. Fang, K. O'Mara, S. Shibayama, S. Piscitelli. 2004. Single and Multiple Dose Escalation Study to Investigate the Safety, Pharmacokinetics, and Receptor Binding of 873140, a Novel CCR5 Receptor Antagonist, in Healthy Subjects 11<sup>th</sup> Conference on Retroviruses and Opportunistic Infections, San Francisco, Abstract 139.
- Demarest,J, S. Shibayama<sup>2</sup>, R. Ferris<sup>1</sup>, C. Vavro<sup>1</sup>, M. StClair<sup>1</sup>, L. Boone<sup>1</sup>. 2004. A Novel CCR5 Antagonist, 873140, Exhibits Potent in vitro Anti-HIV Activity XVII Interscience Conference on Antimicrobial Agents and Chemotherapy, Bangkok, Abstract WeOrA1231,
- Deng H, Unutmaz D, Kewalramani VN and Littman DR (1997) Expression cloning of new receptors used by simian and human immunodeficiency viruses. *Nature* **388**:296-300.
- Doms RW and Peiper SC (1997) Unwelcomed guests with master keys: How HIV uses chemokine receptors for cellular entry *Virology* **235**:179-190.
- Doranz BJ, Rucker J, Smyth Y, Samson RJ, Peiper SC, Parmentier M, Collman RG and Doms RW (1996) A dual-tropic primary HIV-1 isolate that uses fusin and the  $\beta$ -chemokine receptors CKR-5, CKR-3 and CKR-2b as fusion cofactors. *Cell* **85**:1149-1158.

MOL 8685

Doranz BJ, Lu Z-H, Rucker J, Zhang T-Y, Sharron M, Cen Y-H, Wang Z-X, Guo H-H, Du J-D, Accavitti MA, *et. al.* (1997) Two distinct CCR5 domains can mediate coreceptor usage by human immunodeficiency virus type 1 *J Virol* **71**:6305-6314.

Dragic T, Litwin V, Allaway GP, Martin SR, Huang Y, Nagashima KA, Cayan C, Maddon PJ, Koup RA, Moore JP *et. al.* (1996) HIV-1 entry into CD4+ cells is mediated by the chemokine receptor CC CCR-5. *Nature* **381**:667-673.

Dragic T, Trkola A, Thompson DA, Cormier EG, Kajumo FA, Maxwell E, Lin SW, Ying W, Smith SO, Sakmar SP, *et. al.* (2000) A binding pocket for a small molecule inhibitor of HIV-1 entry within the transmembrane helices of CCR5. *Proc Natl Acad Sci U S A* **97**: 5639-5644.

Ehlert F J (1988). Estimation of the affinities of allosteric ligands using radioligand binding and pharmacological null methods. *Mol. Pharmacol.*, **33**,187 – 194

Fillion G, Rouselle, JC, Massot O, Zifa E, Fillion MP and Prudhomme N (1996) A new peptide, 5-HT moduline, isolated and purified mammalian brain specifically interacts with 5-HT1B/1D receptors. *Behav Brain Res.* **73**:313-317.

Finke PE, Oates B, Mills SG, MacCross M, Malkowitz L, Springer MS, Gould SL, DeMartino JA, Carella A, Carver G *et al.* 2001 Antagonists of the human CCR5 receptor as anti-HIV-1 agents. Part 4: synthesis and structure–

MOL 8685

- Activity relationships for 1-[N-(Methyl)-N-(phenylsulfonyl)amino]-2-(phenyl)-4-(4-(N-(alkyl)-N-(benzyloxycarbonyl)amino)piperidin-1-yl)butanes *Bioorg Med Chem Lett* **11**:2475-2479.
- Hall DA (2000) Modeling the functional effects of allosteric modulators at pharmacological receptors: An extension of the two-state model of receptor activation. *Mol Pharmacol* **58**:1412-1423.
- Kazmierski WM, Boone L, Lawrence W, Watson C., Kenakin T CCR5 Chemokine Receptors: Gatekeepers of HIV-1 Infection (2002) *Current Drug Targets - Infectious Disorders*, **2**: 265-278.
- Kazmierski WM, Bifulco N, Yang H, Boone L, DeAnda F, Watson C and Kenakin T (2003) Recent progress in discovery of small-molecule CCR5 Chemokine receptor ligands as HIV-1 inhibitors *Bioorg Med Chem* **11**:2663-2676.
- Kenakin, T.P. (2004a) A Pharmacology Primer; Theory, Application and Methods. Academic Press/ Elsevier.
- Kenakin TP (2004b) Allosteric modulators; the new generation of receptor antagonist. *Molec. Interventions* **4**:222-229.
- Kuhmann SE, Pugach P, Kunstman KJ, Taylor J, Stanfield RL, Snyder A, Strizki JM, Riley J, Baroudy BM, Wilson IA et. al. 2004 Genetic and phenotypic analyses of human immunodeficiency virus type 1 escape from small-molecule CCR inhibitor *J Virol* **78**:2790-2807.



MOL 8685

- Kwong PD, Wyatt R, Robinson J, Sweet RW, Sodroski J and Hendricks W A (1998) Structure of an HIV gp120 envelope glycoprotein in complex with the CD4 receptor and a neutralizing human antibody *Nature* **393**: 648 – 659
- Lee B, Sharron M, Blanpain C, Doranz BJ, Vakili J, Setoh P, Berg E, Liu G, Guy HR, Durell R *et. al.* 1999a Epitope Mapping of CCR5 Reveals Multiple Conformational States and Distinct but Overlapping Structures Involved in Chemokine and Coreceptor Function *J. Biol. Chem.* **274**:9617-9626
- Luckow VA, Lee SC, Barry GF and Olis PO (1993) Efficient generation of infectious recombinant baculoviruses by site-specific transposon-mediated insertion of foreign genes into a baculovirus genome propagated in *Escherichia coli*. *J Virol* **67**: 4566-4579.
- Maeda K, Nakata H, Koh Y, Miyakawa T, Ogata H, Takaoka Y, Shibayama S, Sagawa K, Fukushima D, Moravek J, *et al.* 2004 Spirodiketopiperazine-based CCR5 inhibitor which preserves CC-chemokine/CCR5 interactions and exerts potent activity against R5 human immunodeficiency virus type 1 *in vitro*. *J. Virol.* **78**: 8654-8662.
- Massot O, Rouselle JC, Fillion MP, Grimaldi B, Cloez-Tayarani I, Fugelli A, Prudhomme N, Segun L, Rousseau B, Plantefol M. *et. al.* 1996 5-Hydroxytryptamine-moduline, a new endogenous cerebral peptide, controls the serotonergic activity via its specific interaction with 5-hydroxytryptamine <sub>1B/1D</sub> receptors. *Mol Pharmacol* **50**:752-762.

MOL 8685

O'Reilly DR, Miller LK and Luckow VA (1992) *Baculovirus expression vectors: A laboratory manual*. Oxford University Press, New York.

Palani A, Shapiro S, Clader JW, Greenlee WJ, Cox K, Strizki J, Endres M and Baroudy BH, 2001 Discovery of 4-[(Z)-(4-Bromophenyl)-(ethoxyimino)methyl]-1'-[(2,4-dimethyl-3-pyridinyl)carbonyl]-4'-methyl-1,4'-bipiperidine N-Oxide (SCH 351125): An Orally Bioavailable Human CCR5 Antagonist for the Treatment of HIV Infection *J Med Chem* **44**: 3339-3342

Perros, Manoussos; Price, David Anthony; Stammen, Blanda Luzia Christa; Wood, Anthony, PCT Int. Appl. (2001), WO 2001090106

Picard L, Simmons G, Power CA, Meyer A, Wiess RA and Clapham PR 1997 Multiple extracellular domains of CCR-5 contribute to human immunodeficiency virus type 1 entry and fusion *J. Virol.* **71**: 5003-5011.

Poignard P, Saphire EO, Parren PW, and Burton DR 2001 gp120 :Biologic aspects of structural features. *Annu Rev Immunol* **19** :253-274.

Rizzuto CD, Wyatt R, Hernández-Ramos N, Sun Y, Kwong PD, Hendrickson WA and Sodroski J 1998 A Conserved HIV gp120 Glycoprotein Structure Involved in Chemokine Receptor Binding *Science* **280**: 1949-1953.

Ross T, Bieniasz PD and Cullen BR 1999 Role of chemokine receptors in HIV-1 infection and pathogenesis *Adv. Virus Res* **52**:233-267.

Rucker J, Edinger AL, Sharron M, Samson M, Lee B, Berson JFY, Collman RG, Doranz BJ, Doms RW and Parmentier M 1997 Utilization of chemokine

MOL 8685

- receptors, orphan receptors, and herpesvirus- encoded receptors by diverse human and simian immunodeficiency viruses *J Virol* **71**:8999-9007.
- Sabroe I, Peck MJ, Van Keulen BJ, Jorritsma A, Simmons G, Clapham PR, Williams TJ and Pease JE 2000 A small molecule antagonist of chemokine receptors CCR1 and CCR3. *J Biol Chem* **275**:25985-25992.
- Shieh JTC, Albright AV, Sharron M, Gartner S, Stritzki J, Doms RW and Gonzalez-Scarano F 1998 Chemokine receptor utilization by human immunodeficiency virus type 1 isolates that replicate in microglia. *J Virol* **72**:4243-4249.
- Staudinger R, Wang X, and Bandres JC 2001 Allosteric regulation of CCR5 by guanine nucleotides and HIV-1 envelope. *Biochem Biophys Res Comm* **286**: 41-47.
- Strizki JM, Xu S, Wagner NE, Wojcik L, Liu J, Hou Y, Endres M, Anandan P, Shapiro S, Clader JW, Greenlee WJ *et al* 2001 SCH-C (SCH 351125), an orally bioavailable, small molecule antagonist of the chemokine receptor CCR5, is a potent inhibitor of HIV-1 infection *in vitro* and *in vivo* *Proc. Natl. Acad. Sci. USA*. **98**, 12718-12723.
- Smyth RJ, Yi Y, Singh A and Collman RG 1998 Determinants of Entry Cofactor Utilization and Tropism in a Dualtropic Human Immunodeficiency Virus Type 1 Primary Isolate *J Virol* **72**:4478-4484.
- Tagat JR, McCombie SW, Nazareno D, Labroli MA, Xiao Y, Steensma RW, Strizki JM, Baroudy BM, Cox K, Lachowicz J, Varty G, Watkins R 2004 Piperazine-Based CCR5 Antagonists as HIV-1 Inhibitors. IV. Discovery of

MOL 8685

- 1-[(4,6-Dimethyl-5-pyrimidinyl)carbonyl]-4-[4-{2-methoxy-1(R)-4-(trifluoromethyl) phenyl} ethyl-3(S)-methyl-1-piperazinyl]-4-methylpiperidine (Sch-417690/Sch-D), a Potent, Highly Selective, and Orally Bioavailable CCR5 Antagonist. *J Med Chem* **47**: 2405-2408.
- Trkola A, Kuhmann SE, Strizki JM, Maxwell E, Ketas T, Morgan T, Pugach P, Xu S, Wojcik L, Tagat J, Palani A, Shapiro S, Clader JW, McCombie S, Reyes GR, Baroudy BM, and Moore JP. (2002) HIV-1 escape from a small molecule, CCR5-specific entry inhibitor does not involve CXCR4 use. *Proc. Natl. Acad. Sci. USA* **99**: 395-400.
- Tsamis F, Gavrilov S, Kajumo F, Seibert C, Kuhmann S, Ketas T, Trkola A, Palani A, Clader JW, Tagat JR et. al. (2003) Analysis of the mechanism by which the small molecule CCR5 antagonists SCH-351125 and SCH-350581 inhibit human immunodeficiency virus type-1 entry. *J Virol* **77**:5201-5208.
- Wu L, LaRosa G, Kassam N, Gordon CJ, Heath H, Ruffing N, Chen J, Humblis J, Samson M, Parmentier M, et. al. (1997) Interaction of the chemokine receptor CCR5 with its ligands: multiple domains for HIV-1 gp120 binding and a single domain for chemokine binding. *J Exp Med* **186**:1373-1381.
- Wyatt R and Sodroski J 1998 The HIV-1 envelope glycoproteins: fusogens, antigens, and immunogens. *Science* **280**:1884-1888.

MOL 8685

Zhang Y-J and Moore JP 1999 Will multiple coreceptors need to be targeted by inhibitors of human immunodeficiency virus type 1 entry? *J Virol* 73:3443-3448

MOL 8685

## Legends for Figures

Figure 1. Chemical structures of CCR5 receptor antagonists

Figure 2. Receptor species measured in a binding assay according to the Ehlert (1988) in panel A where both the [AR] and the [ABR] species produce signals or a measured in binding experiments. Dextral displacements of the saturation binding curve (where the radioligand is [A]) are predicted by this model. B. Non-competitive antagonist model (only [AR] species is monitored) where depression of the radioligand saturation binding curve is predicted with no concomitant dextral displacement.

Figure 3. Displacement of  $^{125}\text{I}$ -MIP-1 $\alpha$  by non-radioactive MIP-1 $\alpha$ . A.

Displacement curves: Ordinates: specifically bound (to CCR5 receptor) cpm from  $^{125}\text{I}$ -MIP-1 $\alpha$ . Abscissae: Molar concentrations of non-radioactive MIP-1 $\alpha$

(logarithmic scale). Curves determined for displacement of various concentrations of  $^{125}\text{I}$ -MIP-1 $\alpha$  see legend in panel A for concentrations) B.

Saturation binding curves for  $^{125}\text{I}$ -MIP-1 $\alpha$  in the absence (filled circles) and presence of various concentrations of non-radioactive MIP-1 $\alpha$ : 10 nM (open circles), 30 nM (filled triangles) and 100 nM (open triangles). C. Relationship between observed  $\text{IC}_{50}$  for non-radioactive MIP-1 $\alpha$  displacement of  $^{125}\text{I}$ -MIP-1 $\alpha$  and initial concentration of  $^{125}\text{I}$ -MIP-1 $\alpha$

Figure 4. Displacement of  $^{125}\text{I}$ -MIP-1 $\alpha$  by non-competitive allosteric antagonists.

A. TAK779: Displacement curves: Ordinates: specifically bound (to CCR5 receptor) cpm from  $^{125}\text{I}$ -MIP-1 $\alpha$ . Abscissae: Molar concentrations of non-

MOL 8685

radioactive TAK 779 (logarithmic scale). Curves determined for displacement of various concentration of  $^{125}\text{I}$ -MIP-1 $\alpha$  (see key in panel A for concentrations). B. Saturation binding curves for  $^{125}\text{I}$ -MIP-1 $\alpha$  in the absence (filled circles) and presence of various concentrations of TAK779 :10 nM (open circles), 30 nM (filled triangles) and 100 nM (open triangles). C. Sch-C. Displacement curves by Sch-C for concentrations of  $^{125}\text{I}$ -MIP-1 $\alpha$  as given in A. D. Saturation binding curves for  $^{125}\text{I}$ -MIP-1 $\alpha$  in the absence (filled circles) and presence of various concentrations of Sch-C (same key as panel A for concentrations). E. Sch-D. Displacement curves by Sch-D for concentrations of  $^{125}\text{I}$ -MIP-1 $\alpha$  as given in A. D. Saturation binding curves for  $^{125}\text{I}$ -MIP-1 $\alpha$  in the absence (filled circles) and presence of various concentrations of Sch-D :3 nM (open circles), 10 nM (filled triangles) and 30 nM (open triangles). G. UK-427,857: Displacement curves by UK-427,857 for concentrations of  $^{125}\text{I}$ -MIP-1 $\alpha$  (see key). H. Saturation binding curves for  $^{125}\text{I}$ -MIP-1 $\alpha$  in the absence (filled circles) and presence of various concentrations of UK-427,857 :3 nM (open circles), 10 nM (filled triangles) and 30 nM (open triangles).

Figure 5. Relationship between the  $\text{IC}_{50}$  for blockade of  $^{125}\text{I}$ -MIP-1 $\alpha$  binding (ordinates) and concentration of radioligand (abscissae). Symbols: MIP-1 $\alpha$  (filled circles), TAK779 (squares), Sch-C (open circles), Sch-D (triangles) and UK 427,857 (diamonds)

Figure 6. Displacement of  $^{125}\text{I}$ -MIP-1 $\alpha$  by 873140. A: Displacement curves: Ordinate: specifically bound (to CCR5 receptor) cpm from  $^{125}\text{I}$ -MIP-1 $\alpha$ .

MOL 8685

Abscissae: Molar concentrations of non-radioactive 873140 (logarithmic scale). A. Displacement curves for 873140 for concentrations of  $^{125}\text{I}$ -MIP-1 $\alpha$  as shown in key. B. Saturation binding curves for  $^{125}\text{I}$ -MIP-1 $\alpha$  in the absence (filled circles) and presence of various concentrations of 873140 (see key) C. Relationship between the  $\text{IC}_{50}$  for blockade of  $^{125}\text{I}$ -MIP-1 $\alpha$  binding (ordinates) and concentration of radioligand (abscissae).

Fig 7. Displacement of  $^{125}\text{I}$ -RANTES from CCR5. Ordinates cpm for specifically bound  $^{125}\text{I}$ -RANTES expressed as a percentage of initial value (740 cpm). Abscissae: logarithms of molar concentrations of antagonist. A. Data shown for UK-427,857 (filled circles, n=4), Sch-D (open circles, n=4), TAK779 (filled squares, n=4) and 873140 (open squares, n=4). Bars represent S.E.M. B. Estimated dextral displacement of the saturation curve for  $^{125}\text{I}$ -RANTES (from  $B_0$  value for panel A shown as open circle) produced by maximal concentrations (1  $\mu\text{M}$ ) of 873140 (open triangle) and Sch-D (filled square). These displacements predict co-operativity constants ( $\alpha$ ) for both antagonists and RANTES (see Appendix 1). Minimal effects on RANTES binding are produced by 873140 while a minimal value for the displacement by Sch-D is shown.

Fig 8. Reversal of blockade by MIP-1 $\alpha$  and allosteric antagonists with time. Ordinates: Natural logarithm of the percent receptor occupancy by the antagonist normalized to 100% at time zero. Abscissae: time in hours. A. Membranes incubated with 1 nM  $^{125}\text{I}$ -MIP-1 $\alpha$  in the presence of non-radioactive MIP-1 $\alpha$  (200 nM), Sch-C (100 nM), 873140 (100 nM) and TAK779 (200 nM).



MOL 8685

Preparations were then washed for 1 to 5 hours as shown and the binding of  $^{125}\text{I}$ -MIP-1 $\alpha$  measured. Key shows symbols for antagonist data. B. Similar protocol as for A except longer wash times were used. Key shows symbols for antagonists; Data describing regressions shown in Table 2.

Fig 9. Calcium responses to chemokine agonists RANTES (panels A to E) and MIP-1 $\alpha$  (panel F). Ordinates: Percent of maximal response to the agonist.

Abscissae: Logarithms of molar concentration of agonist. A. Responses in the absence (filled circles, n=4) and presence of TAK 779 3 nM (open circles), 10 nM (open triangles), and 30 nM (filled squares) (n=4). A. Responses in the absence (filled circles) and presence of Sch-C 10 nM (open circles), 30 nM (filled triangles), and 100 nM (open triangles) (n=3). C. Responses in the absence (filled circles) and presence of Sch-D 3 nM (open circles), 10 nM (open triangles), and 30 nM (filled squares) (n=5). D. Responses in the absence (filled circles, n=4) and presence of UK-427,857 0.3 nM (open circles), 1 nM (open triangles), 3 nM (filled squares) and 10nM (open squares) (n=4). E. Responses in the absence (filled circles) and presence of 873140 1 nM (open circles), 3 nM (filled triangles), and 10 nM (open triangles) (n=3). F. Responses to MIP-1 $\alpha$  in the absence (filled circles) and presence of 873140 1 nM (open circles), 3 nM (filled triangles), and 10 nM (open triangles) (n=5).

Figure 10. Co-administration of two allosteric modulators (a test and reference antagonist respectively). Ordinates; relative initial level of binding of the tracer in the presence of the test antagonist (as a fraction of the initial level of binding in

MOL 8685

the absence of any antagonist). Abscissae; the ratio of the  $IC_{50}$  values of the reference antagonist (for displacement binding) in the presence of various concentrations of test antagonist. Both ordinate and abscissal scales are logarithmic. Model described fully in Appendix 1.

Figure 11. Displacement of bound  $^{125}I$ -MIP-1 $\alpha$  by 873140 in the absence (filled circles) and presence of a test antagonist. Keys show concentrations of antagonists. A. Test antagonist is TAK779. B. Regression of basal binding levels of  $^{125}I$ -MIP-1 $\alpha$  (ordinates) and observed potency (log  $IC_{50}$  values) of 873140 according to equation 12. Solid line represents best linear least squares fit of datapoints and dotted line a line of slope equal to -1. Data characterizing regression shown in Table 3. C. Test antagonist is Sch-C. D. Regression according to equation 12 as for panel B for Sch-C; data describing regression shown in Table 3. E. Test antagonist is Sch-D. F. Regression according to equation 12 as for panel B for Sch-D; data describing regression in Table 3. G. Test antagonist is UK-427,857. H. Regression according to equation 12 as for panel B for UK-427,857 data describing regression in Table 3.

MOL 8685

## Tables

**Table 1**

**Equilibrium Dissociation Constants for Antagonist-CCR5 receptor complexes  
as measured by Displacement or Modification of  $^{125}\text{I}$ -MIP-1 $\alpha$  Binding**

<b>Ligand</b>	<b>K<sub>B</sub> (nM) (95% confidence limits)</b>
<b>MIP-1<math>\alpha</math></b>	8.0 $\pm$ 1.2 (4.7 to 11.2)
<b>TAK779</b>	15.8 (7.9 to 31.6)
<b>Sch-C</b>	6.3 (4 to 10)
<b>Sch-D</b>	4.0 (2.5 to 6.3)
<b>UK-427,857</b>	2.0 (1.2 to 3.1)
<b>873140</b>	2.5 (1.6 to 3.2)

**Table 2**

**Time Course for Reversal of Blockade of  $^{125}\text{I}$ -MIP-1 $\alpha$  Binding**

<b>Non-radioactive Ligand</b>	<b><math>k_{\text{off}}</math> (h<math>^{-1}</math>)</b>	<b>95% c.l.<sup>1</sup></b>	<b>t-value</b>	<b>Signif.<sup>2</sup></b>
<b>MIP-1<math>\alpha</math></b>	0.26 <sup>1</sup>	0.22 to 0.29	8.94 d.f.=36	p<0.005
<b>Sch-C</b>	0.013	0.008 to 0.018	3.73 d.f.=34	p<0.005
<b>Sch-D</b>	0.005	0.004 to 0.006	4.45 d.f.=34	p<0.005
<b>TAK-779</b>	0.013	0.01 to 0.015	5.6 d.f.= 38	p<0.005
<b>UK-427,857</b>	0.0036	0.0026 to 0.0045	3.78 d.f.=41	p<0.005
<b>873140</b>	-----	-----	0.93 d.f.=41	n.s

<sup>1</sup> 95% confidence limits of the slope from a plot of ln (receptor occupancy) vs time (h).

<sup>2</sup> value of t to determine if a significant dependence of antagonist receptor occupancy exists on time, i.e. if washing with drug free media causes reduction in the receptor occupancy by the antagonist. Insignificant values of t indicate no relationship between time and occupancy, i.e. operationally an irreversible receptor occupancy by the antagonist over the time period of the experiment, specifically 51 h.

<sup>3</sup>This value obtained at room temperature. All other values obtained at 4 °C. No reversal of receptor occupancy was observed at room temperature for other antagonists at wash periods up to 8 h.

**Table 3**

**Relationship between potency of 873140 in the presence of test antagonists**

<b>Test Antagonist</b>	<b>Tvalue<sup>1</sup></b>	<b>Significance</b>	<b>Slope<sup>2</sup></b>	<b>95% Confidence Limits of Slope</b>
<b>TAK 779</b>	8.17	p<0.0005	-0.84	-1.1 to -0.55
<b>Schering-C</b>	14.2	p<0.0005	-1.18	-1.1 to -0.9
<b>Schering-D</b>	15.1	p<0.0005	-1.1	-1.3 to -0.84
<b>UK-427,857:</b>	14.8	p<0.0005	-1.0	-1.3 to -0.8

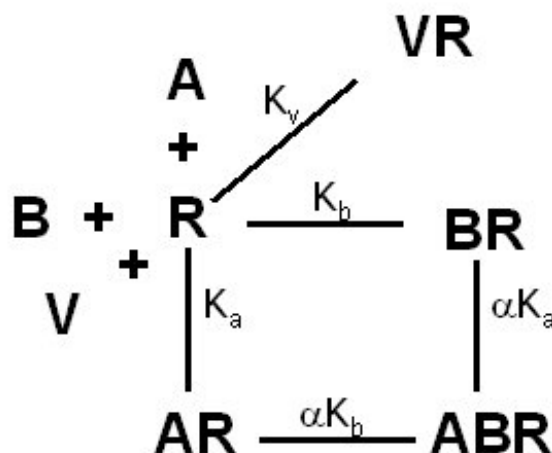
<sup>1</sup> measure of the significance of a possible relationship between x and y values. In this case x is the log of the ratio of IC<sub>50</sub> values for the reference antagonist in the presence and absence of test antagonist (ordinates for fig 8)- and y is the log of the ratio of B<sub>0</sub> values in the presence and absence of test antagonist (ordinates for fig 8)-see Methods for further details.

<sup>2</sup> Slope of the regression of x and y as shown in fig 8.

## Appendix 1: Three Ligand Interactions

### A. Allosteric Non-Competitive Interactive

Receptor [R] interacts with virus ([V]), and 2 non-competitive ligands [A] and [B]. Each antagonist binds to its own binding site and the binding of one allosteric antagonist affects the binding of the other by a co-operativity factor  $\alpha$ .



$$[AR] = [ABR]/(\alpha[B]K_b) \quad \dots[14]$$

$$[BR] = [ABR]/(\alpha[A]K_a) \quad \dots[15]$$

$$[R] = [ABR]/(\alpha[A]K_a[B]K_b) \quad \dots[16]$$

The occupancy by antagonists A and B as a fraction of total receptor occupancy (converting association equilibrium constants  $K_a$  and  $K_b$  to dissociation constants) is given by:

$$\rho_{AB} = \frac{[A]/K_A (1 + \alpha[B]/K_B) + [B]/K_B}{[A]/K_A (1 + \alpha[B]/K_B) + [B]/K_B + 1} \quad \dots[17]$$

The fractional occupancy by tracer (such as  $^{125}\text{I}$ -MIP-1 $\alpha$ ) is given by:

MOL 8685

$$\rho_t = \frac{[\text{tracer}]/K_t}{([\text{tracer}]/K_t) + 1} (1 - \rho_{\text{Antagonist}}) \quad \dots[18]$$

where  $\rho_{\text{Antagonist}}$  is the fractional receptor occupancy by the non-competitive antagonist. From mass action for receptor occupancy by antagonist [A]:

$$(1 - \rho_A) = (1 + [A]/K_A)^{-1} \quad \dots[19]$$

Similarly, from equation 17:

$$(1 - \rho_{AB}) = ([A]/K_A (1 + \alpha[B]/K_B) + [B]/K_B + 1)^{-1} \quad \dots[20]$$

The occupancy of the receptor by a tracer molecule at any concentration [tracer] is given by equation 17. Comparing receptor occupancy for a tracer in the presence of antagonist [A] as a fraction of the occupancy of the tracer in the absence of [A] and letting [A] equal the  $IC_{50}$  of the test antagonist [A] yields:

$$0.5 = \frac{1 + [IC_{50}]/K_A}{[IC_{50}]/K_A (1 + \alpha[B]/K_B) + [B]/K_B + 1} \quad \dots[21]$$

which leads to

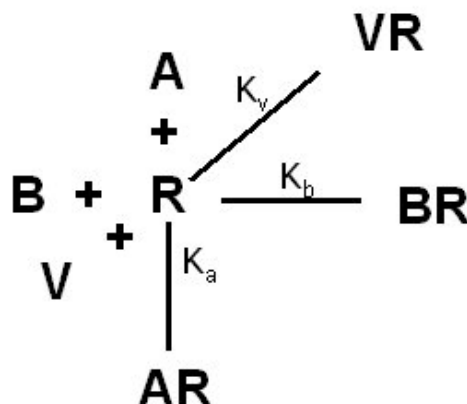
$$\frac{IC_{50}}{K_A} = \text{Ratio}_I = \frac{(1 + [B]/K_B)}{(1 + \alpha[B]/K_B)} \quad \dots[22]$$

It can be seen that if the sites are mutually exclusive (either binding of A precludes the binding of B and vice versa such as would be obtained with a single binding site for both) then  $\alpha = 0$ . This can be shown independently as shown below.

## B. Allosteric Non-Competitive Non-Interactive

MOL 8685

Receptor [R] interacts with virus ([V]), and 2 non-competitive ligands [A] and [B] such that the binding of A precludes binding of B and vice versa.



$$[R] = [AR]/[A]K_a \quad \dots[23]$$

$$[BR] = [B]K_b[AR]/[A]K_a \quad \dots[24]$$

Fractional receptor occupancy by [A] and [B] is given by:

$$\rho = [AR]+[BR]/([AR]+[BR]+[R]) \quad \dots[25]$$

Converting association equilibrium constants  $K_a$  and  $K_b$  to dissociation constants this is given by:

$$\rho_{AB} = \frac{[A]/K_A + [B]/K_B}{[A]/K_A + [B]/K_B + 1} \quad \dots[26]$$

The fractional occupancy by virus is given by:

$$\rho_V = \frac{[V]/K_V}{[V]/K_V + 1} (1-\rho_{\text{Antagonist}}) \quad \dots[27]$$



MOL 8685

where  $\rho_{\text{Antagonist}}$  is the fractional receptor occupancy by the non-competitive antagonist. The  $IC_{50}$  for antagonist [A] is given by the ratio of tracer occupancy in the presence of both A+B and B:

$$IC_{50} = \frac{\rho_t(1-\rho_{AB})}{\rho_t(1-\rho_B)} = K_A (1 + [B]/K_B) \dots [28]$$

It can be seen that equation 28 is equation 22 when  $\alpha=0$  in accordance with the fact that  $\alpha=0$  represents the special case where there is no interaction between ligands A and B in the interactive model.

### C. Relationship between $B_0$ and $IC_{50}$ with Antagonist Co-administration

Equation 22 can be used to determine the relationship between the effect of the test antagonist on resting level of radioligand binding and observed potency of the reference antagonist obtained in the presence of various concentrations of test antagonist.

The bound basal tracer binding in the absence of the test antagonist is defined as  $B_0$  and is given by mass action:

$$B_0 = \frac{[\text{tracer}]}{[\text{tracer}] + K_d} \dots [29]$$

where  $K_d$  is the equilibrium dissociation constant of the tracer molecule-receptor complex. The binding in the presence of a pre-equilibrated concentration of test non-competitive antagonist is defined as  $B'_0$  and is given as:

$$B'_0 = \frac{[\text{tracer}]}{[\text{tracer}] + K_d} (1 - \rho_{\text{Antagonist}}) \dots [30]$$

where  $\rho_{\text{Antagonist}}$  is the fractional receptor occupancy by the antagonist given by:

$$\rho_{\text{Antagonist}} = \frac{[B]/K_B}{[B]/K_B + 1} \quad \dots[31]$$

The ratio of tracer binding levels in the presence and absence of the non competitive antagonist is given by  $B'_0/B_0$  and, substituting from equation 31, it can be shown that:

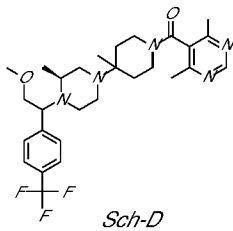
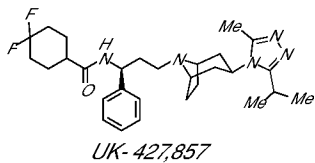
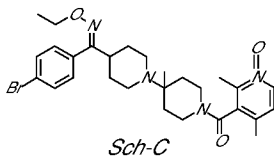
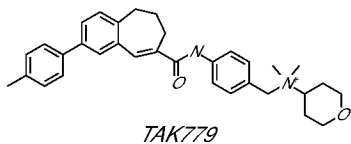
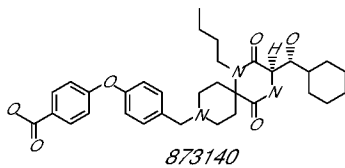
$$\frac{[B]}{K_B} = \frac{(1 - (B'_0/B_0))}{B'_0/B_0} \quad \dots[32]$$

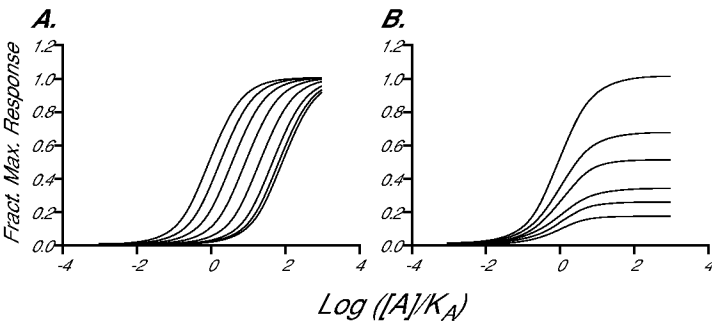
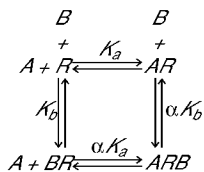
Substituting for  $[B]/K_B$  in equation 22 yields:

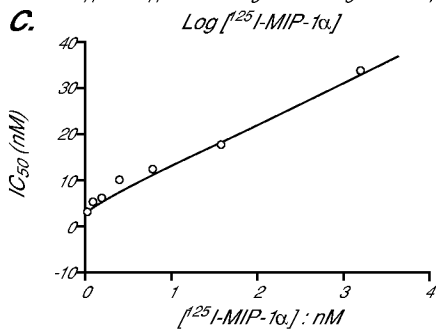
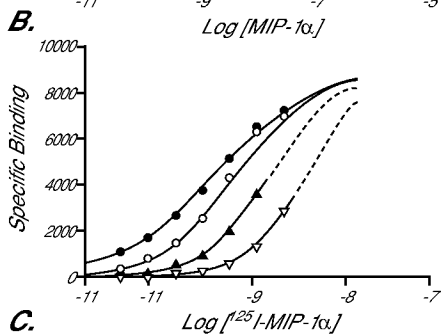
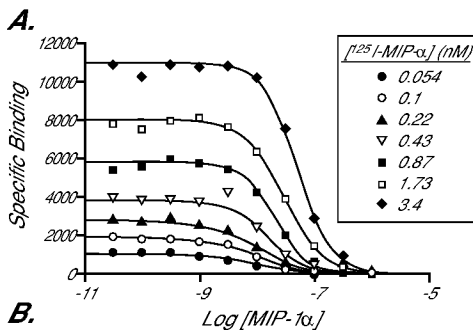
$$\frac{B'_0}{B_0} = \frac{K_A}{IC_{50} (1 - \alpha)} + \frac{\alpha}{(1 - \alpha)} \quad \dots[33]$$

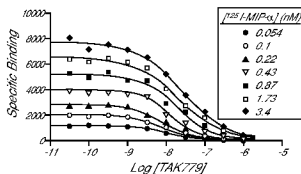
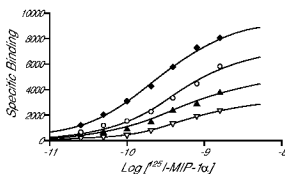
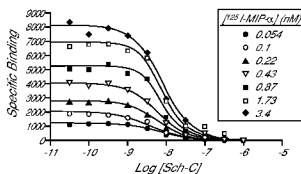
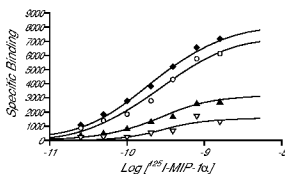
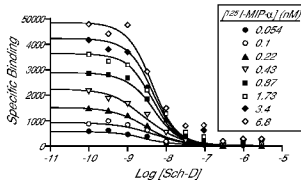
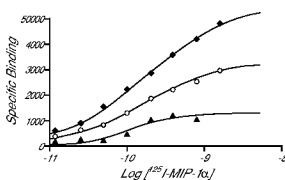
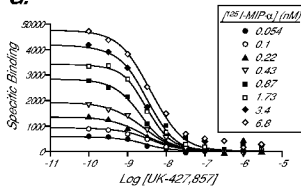
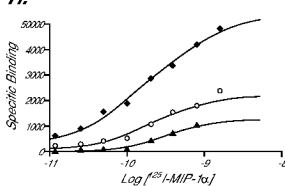
It can be seen from equation 33 that when  $\alpha=0$  (both antagonists bind to a common site or the binding of one antagonist precludes binding of the other at the same time), the logarithmic metameter yields a straight line with a slope of negative one:

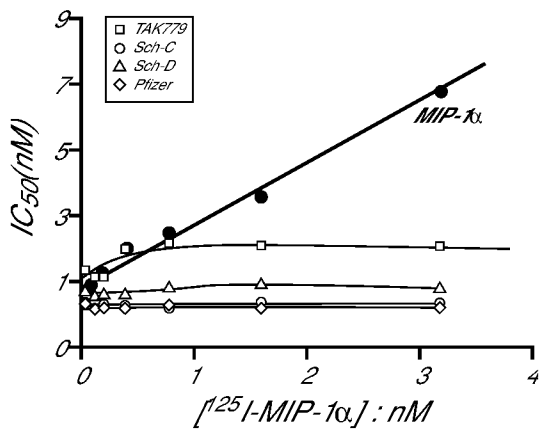
$$\text{Log } (B'_0/B_0) = -\text{Log } (IC_{50}/K_A) \quad \dots[34]$$

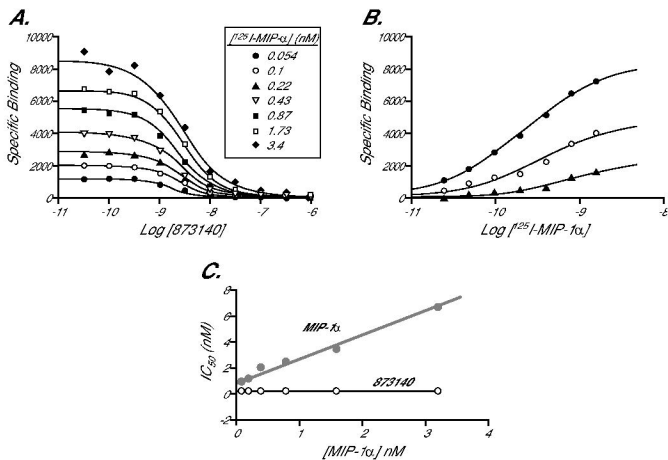




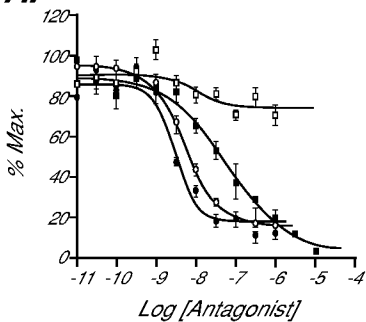
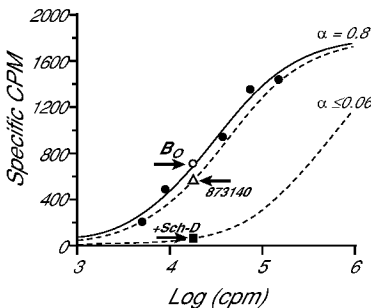


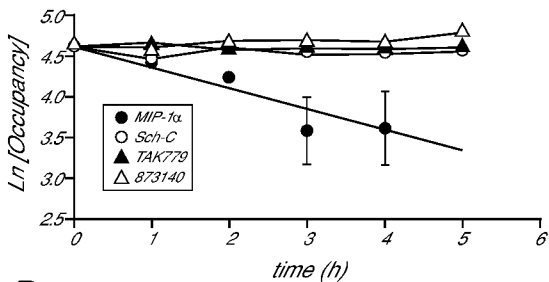
**A.****B.****C.****D.****E.****F.****G.****H.**







**A.****B.**

**A.****B.**